Estimation of Lower-Body Kinetics from Loading Profile and Kinematics Alone, Without Measured Ground Reaction Forces

William K. Thompson[1], Christopher A. Gallo[2], Beth E. Lewandowski[3]
NASA Glenn Research Center, 21000 Brookpark Rd., Cleveland, OH 44135

R. Kenneth Huffman[4]
Metecs, Inc., 1030 Hercules Ave., Houston, TX 77058

Bradley T. Humphreys[5], Aaron P. Godfrey[6]
ZIN Technologies, 6745 Engle Road, Airport Executive Park, Cleveland, OH 44130

David Frenkel[7]
CACI, Inc., 2100 Space Park Dr., Houston, TX 77058

John K. DeWitt[8]
KBRWyle, 2400 NASA Parkway, Houston, TX 77058

Biomechanical models of human motion can estimate kinetic outcomes, such as joint moments, joint forces, and muscle forces. Typically, one performs an inverse dynamics (ID) analysis to compute joint moments from the kinematics and measured external forces. Sometimes it is impractical to measure ground reaction forces and moments (GRF&M). We devised an empirical method for performing ID analysis of resistance exercises without measured GRF&M. The method solves the multibody dynamics equations of motion with four key assumptions about the GRF&M that reduce the number of unknowns. The assumptions are 1) negligible ground reaction moments, 2) fixed lateral/medial location of the center of pressure (COP), 3) equal fore/aft location of the COP between the feet, and 4) constant angle of the GRF vector relative to vertical in the frontal plane. We used evaluation trials from a prototype exercise countermeasure device to test this approach. Four participants performed squat and deadlift exercises at various loads. We compared results from traditional ID analysis to results without measured GRF&M using our method. We found that joint moment trajectories in the sagittal plane were similarly shaped between the two methods, and the amount of root mean squared error (RMSE), measured by difference in joint moment impulse, was typically under 15% (except for deadlift at the knee, <50%). Non-sagittal joint moment trajectories, which are much lower in overall magnitude, were not always similarly shaped between the two methods. Non-sagittal moments displayed much higher RMSE, with values ranging from 50-1000%. These findings were further supported by validation metrics (Sprague and Geers' *P* and *M* metrics, Pearson's *r* correlation coefficient). Based on these findings, we concluded that useful kinetic results are obtained from ID analysis of squat and deadlift exercises, even without measuring GRF&M, as long as the outcomes of interest lie in the sagittal plane.

[1] Research Biomedical Engineer, Fluid Physics and Transport Processes Branch.
[2] Research Mechanical Engineer, Mechanical Systems Design and Integration Branch.
[3] Project Scientist, Fluid Physics and Transport Processes Branch.
[4] Senior Systems Engineer, R&D and Business Development.
[5] Dynamics and Controls Engineer, Mechanical Analysis Group.
[6] Physicist II, Human Research Program.
[7] Aerospace Engineer, EIT Group.
[8] Senior Biomechanist, Health and Human Performance Directorate.

Nomenclature

$\boldsymbol{a}$	=	system acceleration
CM_{sys}	=	system center of mass
d	=	fixed distance
$\boldsymbol{F}$	=	force vector
$\boldsymbol{F}_b$	=	externally applied bar force from tethered cable
$\boldsymbol{F}_d$	=	externally applied device force
$\boldsymbol{F}_{est}$	=	estimated external force
$\boldsymbol{F}_h$	=	externally applied harness force from tethered cable
$\boldsymbol{F}_L$	=	ground reaction force on left foot
$\boldsymbol{F}_R$	=	ground reaction force on right foot
$\boldsymbol{F}_{meas}$	=	measured force
$\boldsymbol{H}$	=	system angular momentum matrix
M	=	magnitude difference metric (between trajectories)
m	=	system mass
$\boldsymbol{M}$	=	moment vector
$\boldsymbol{M}_{est}$	=	estimated moment
$\boldsymbol{M}_L$	=	ground reaction moment on left foot
$\boldsymbol{M}_R$	=	ground reaction moment on right foot
$\boldsymbol{M}_{meas}$	=	measured moment
M_Y	=	Y component of ground reaction moment, i.e., "free moment"
n	=	an integer
P	=	curve phase difference metric (between trajectories)
$\boldsymbol{r}$	=	point of application of a force
$\boldsymbol{r}_d$	=	point of application of device force
$\boldsymbol{r}_L$	=	COP vector from system COM to $\boldsymbol{F}_L$
$\boldsymbol{r}_R$	=	COP vector from system COM to $\boldsymbol{F}_R$
r_b	=	point of application of tension force from harness
θ	=	angle of the GRF vector with the vertical axis in the *YZ* plane
API	=	Application Programming Interface
BH	=	body height (in meters)
BWF	=	body weight force (in Newtons)
CCMP	=	Cross-cutting Computational Modeling Project
COM	=	center of mass
COP	=	center of pressure
DART	=	Device for Aerobic and Resistive Training
ECL	=	Exercise Countermeasures Laboratory
F1, F2	=	flywheel exercise loading trials
FW	=	free weight loading profile
FLY	=	flywheel loading profile
GRF	=	ground reaction force
GRF&M	=	ground reaction forces and moments
H	=	heavy FW trial
HHC	=	Human Health and Countermeasures
HRP	=	Human Research Program
ID	=	inverse dynamics
IMS	=	inertial measurement sensor
L	=	light FW trial
LHS	=	left hand side (of equation)
M	=	medium FW trial
POA	=	point of application (of external force)
RHS	=	right hand side (of equation)
*n*RM	=	*n*-repetition maximum
RMSE	=	root mean squared error
SD	=	standard deviation
ZMP	=	zero moment point

I. Introduction

Biomechanical models can estimate kinetic outcomes, such as joint moments, joint forces, and muscle forces during human motion. Following data collection, one typically performs an inverse dynamics (ID) analysis to compute joint moments from the motion-derived kinematics and the measured external forces applied during the activity. This procedure allows for computing the system kinetics by solving the Newton-Euler equations of motion directly to obtain the generalized forces and moments.

Sometimes it is not practical to measure the ground reaction forces and moments (GRF&M), despite the fact that traditional ID requires knowledge of all external forces acting on the body. Reasons for not measuring the GRF&M usually arise from practical considerations such as cost, spatial constraints precluding the appropriate placement of force plates, or the inability to study the movement in a laboratory setting at all. For our particular research interest, human spaceflight, the additional factors of upmass and increased operational complexity are also considerations.

Various methods exist in the literature for estimating system kinetics without measuring the GRF&M using force plates. These methods may involve the use of alternative, lower-cost, less-burdensome sensors such as foot pressure sensors [1,2,3] or inertial measurement sensors (IMS) [4,5,6], which can provide a subset of the GRF&M components to reduce the indeterminacy. More analytical methods may employ optimization techniques [7], contact surface models [8], or both [9,10]. A less-commonly reported method involves the use of simplifying assumptions based on empirical knowledge of the motion under study to reduce the number of unknowns. This type of method has been explored for gait[11] using a smooth transition assumption to fit measured force plate data to empirically determined analytical functions, and we aim to develop an analogous empirical methodology for the squat and deadlift. These exercises promote general health and fitness, both terrestrially and during human spaceflight [12,13].

This work proposes a practical method for performing ID analysis to study whole-body resistance training kinetics without measuring GRF&M. The method is similar to the zero moment point (ZMP) method used in a previous gait study[14], but it deviates from ZMP by making four specific key assumptions about the GRF&M that reduce the indeterminacy. These assumptions arise from empirical observations that are quite specific to the squat and deadlift exercises in the laboratory. The method first estimates the missing components of the GRF&M and then performs a traditional ID analysis using these estimated values, all without modifying the model, without coding optimization algorithms, and without introducing complex contact surfaces at the feet.

A. Force Balance Techniques

Laboratory biomechanical studies typically quantify the kinematics of human body segments using motion capture techniques. Direct measurement of all external forces, points of application (POAs) of forces, and moments on the human body system and/or exercise device components may also be measured. From this information, multibody ID formulations can be employed to determine the human system kinetics (generalized forces and moments at each joint).

In the case where a subset of the existing external forces and/or moments are not directly measured (e.g., the GRF&Ms), it is sometimes possible to estimate the unmeasured forces, moments, and/or POAs using basic force and moment balance techniques. Those values are then used in the multibody formulations discussed above to calculate the system kinetics. Referring to Figure 1, the general force and moment balance equations, rearranged with estimated quantities on the left and with known or measured quantities on the right, appear as:

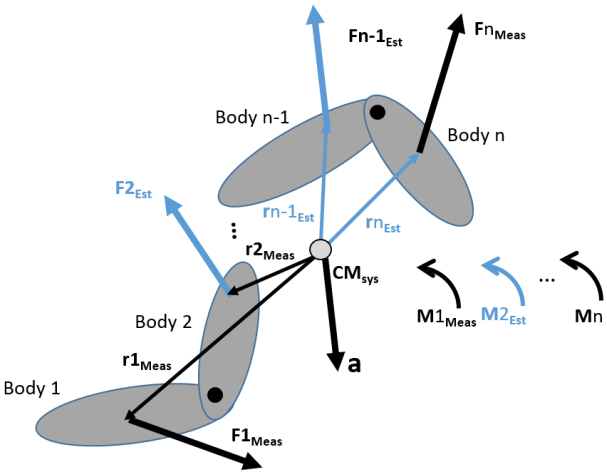

Figure 1. Multibody system with measured and estimated (i.e., unmeasured) forces, moments, and POA.

$$\sum \boldsymbol{F}_{est} = m\boldsymbol{a} - \sum \boldsymbol{F}_{meas} \tag{1}$$

$$\sum(\boldsymbol{r} \times \boldsymbol{F})_{est} + \sum \boldsymbol{M}_{est} = \frac{d\boldsymbol{H}}{dt} - \sum(\boldsymbol{r} \times \boldsymbol{F})_{meas} - \sum \boldsymbol{M}_{meas} \tag{2}$$

where:

m = total system mass
$\boldsymbol{a}$ = acceleration of the system COM (CM_{sys})
r = position vector of POA
$d\boldsymbol{H}/dt$ = rate of change of system angular momentum about the system COM
$\boldsymbol{F}_{meas}$, $\boldsymbol{M}_{meas}$, $(\boldsymbol{r}\times\boldsymbol{F})_{meas}$ = measured external forces, moments, cross product moments
$\boldsymbol{F}_{est}$, $\boldsymbol{M}_{est}$, $(\boldsymbol{r}\times\boldsymbol{F})_{est}$ = estimated external forces, moment to be estimated, cross product moments

The forces, moments, and POAs on the right hand sides (RHSs) of Eq. (1) and (2) are known by direct measurement. The RHS momentum terms can be calculated from the motion capture supplied kinematics and the mass properties of the human body segments. Segment mass properties are determined by scaling the base models[19] to the participants' measured anthropometrics. If the subset of unmeasured forces, moments, and POAs is limited enough, these equations can be solved, and the unmeasured quantities on the left hand sides (LHSs) of Eq. (1) and (2) can be estimated directly. If, however, the number of unknowns on the LHS exceeds the number of independent relationships, the unmeasured elements cannot be solved for straightaway, but may still be estimated if reasonable simplifying assumptions can be made to reduce the number of unknowns.

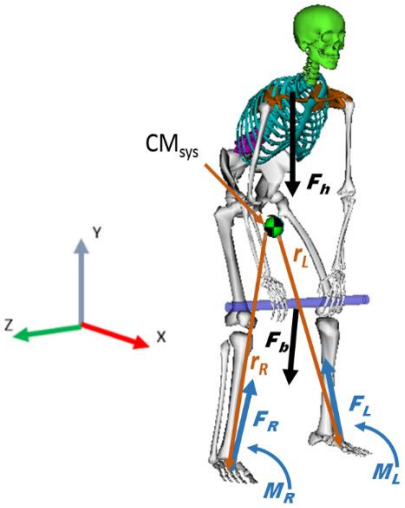

Figure 2. External forces (F_R and F_L) and moments (M_R and M_L) on the human system: for deadlift, using a bar, F_b; and for squat, using a harness, F_h.

B. Simplifying Assumptions for Squat and Deadlift Exercises

These assumptions are based on limited empirical evidence that we have gathered in our laboratory while studying the kinematics and kinetics of over 100 squat and deadlift trials. We have studied these exercises in the context of spaceflight exercise countermeasure device development with a traditional marker-based motion capture system. (See the Methods for a detailed description of the exercise countermeasure device.) The methodology is as follows:

Referring to Figure 2, Eq. (1) and (2) can be written with estimated quantities on the LHS and measured or known quantities on the RHS for the specific cases in this work as:

$$\boldsymbol{F}_L + \boldsymbol{F}_R = m\boldsymbol{a} - m\boldsymbol{g} - \boldsymbol{F}_d \tag{3}$$

$$\boldsymbol{r}_L \times \boldsymbol{F}_L + \boldsymbol{r}_R \times \boldsymbol{F}_R + \boldsymbol{M}_L + \boldsymbol{M}_R = \frac{d\boldsymbol{H}}{dt} - \boldsymbol{r}_d \times \boldsymbol{F}_d \tag{4}$$

where:

$\boldsymbol{F}_d$ = device force (bar force, $\boldsymbol{F}_b$, for deadlift trials or harness force, $\boldsymbol{F}_h$, for squat trials)
$\boldsymbol{F}_L$, $\boldsymbol{F}_R$, $\boldsymbol{M}_L$, $\boldsymbol{M}_R$ = left, right GRF&M
$m\boldsymbol{g}$ = total gravitational force
$\boldsymbol{r}_d$ = POA vector from system COM to $\boldsymbol{F}_d$
$\boldsymbol{r}_L$, $\boldsymbol{r}_R$ = POA vectors from system COM to $\boldsymbol{F}_L$, $\boldsymbol{F}_R$

We assume that the bar and device tether (or harness and device tether) are connected by a frictionless spherical joint, with no net moment.

Even a cursory review of Eq. (3) and (4) reveals that there are substantially more unknowns than independent equations. Therefore, the direct calculation of unmeasured GRF&Ms and their POAs is not possible without the additional simplifying assumptions.

The first assumption is that the moments at the feet are negligible enough to be set to zero. In the case of the *X* and *Z* components, this is truly the case, as without foot restraints, pure couples in those directions are not realizable. It is possible to generate a pure couple in the *Y* direction by twisting the foot on the plate, but we assume it to be small.

With this assumption, Eq. (4) reduces to:

$$\boldsymbol{r}_L \times \boldsymbol{F}_L + \boldsymbol{r}_R \times \boldsymbol{F}_R = \frac{d\boldsymbol{H}}{dt} - \boldsymbol{r}_d \times \boldsymbol{F}_d \tag{5}$$

and solving Eq. (3) for $\boldsymbol{F}_R$, substituting the result in Eq. (5), and rearranging yields:

$$(\boldsymbol{r}_L - \boldsymbol{r}_R) \times \boldsymbol{F}_L = \frac{d\boldsymbol{H}}{dt} - \boldsymbol{r}_d \times \boldsymbol{F}_d - \boldsymbol{r}_R \times (m\boldsymbol{a} - m\boldsymbol{g} - \boldsymbol{F}_d) \tag{6}$$

Note that the Y component of $\boldsymbol{r}_L$ and $\boldsymbol{r}_R$ must be the foot contact surface height (a known quantity), and that the component of $\boldsymbol{F}_L$ parallel to $\boldsymbol{r}_L - \boldsymbol{r}_R$ does not factor in Eq. (6). The six remaining unknowns are the X and Z components of $\boldsymbol{r}_L$ and $\boldsymbol{r}_R$, and the two components of $\boldsymbol{F}_L$ that are perpendicular to $\boldsymbol{r}_L - \boldsymbol{r}_R$. Since Eq. (6) represents three independent equations, three additional assumptions are required.

The second assumption is that the Z components of $\boldsymbol{r}_L$ and $\boldsymbol{r}_R$ are a fixed distance (2 cm) outside the centerline of the feet as shown in Figure 3. Similarly motivated, the third assumption is that the X components of $\boldsymbol{r}_L$ and $\boldsymbol{r}_R$ are equal, also shown in Figure 3. The fourth assumption requires the introduction of an angle θ that $\boldsymbol{F}_L$ makes with the YZ plane as shown in Figure 4. The assumption is that θ remains constant through the exercise, with a value of 8.6°. These assumptions, and their chosen values, were empirically determined from observing over 100 squat and deadlift trials across the four participants in our laboratory based on composite averages of the measured GRF POAs and angle with the XY plane. The vectors in (6) that are affected by assumptions 2, 3 and 4 are $\boldsymbol{r}_L$, $\boldsymbol{r}_R$, and $\boldsymbol{F}_L$. The components of these vectors, as they relate to the assumptions, can be written explicitly as detailed below.

Introduce the vectors $\boldsymbol{F}_T = m\boldsymbol{a} - m\boldsymbol{g} - \boldsymbol{F}_d$ and $\boldsymbol{M}_T = d\boldsymbol{H}/dt - \boldsymbol{r}_d \times \boldsymbol{F}_d$. These vectors represent the total force and moment required for balance, and are known quantities. Also introduce $\boldsymbol{r}_{Lcm}$ and $\boldsymbol{r}_{Rcm}$ as the vectors from the CM_{sys} to the left and right foot center of masses, again these are known from kinematics. Similarly, designate d_{TP} as the distance from the CM_{sys} to the top of the force plate, which is also known. The components of $\boldsymbol{r}_L$, $\boldsymbol{r}_R$, and $\boldsymbol{F}_L$ can then be written as:

$$\begin{aligned} r_{LX} &= r_{RX} = (M_{TZ} + d_{TP}F_{TX})/F_{TY} \textbf{ (Assumption 3)} \\ r_{LY} &= r_{RY} = d_{TP} \\ r_{LZ} &= r_{LcmZ} - (2\text{ cm}) \textbf{ (Assumption 2)} \\ r_{RZ} &= r_{RcmZ} + (2\text{cm}) \textbf{ (Assumption 2)} \end{aligned} \tag{7}$$

$$\begin{aligned} F_{LX} &= (M_{TY} + r_{LX}F_{TZ} - r_{RZ}F_{TX}))/(r_{LZ} - r_{RZ}) \\ F_{LY} &= (d_{TP}F_{TZ} - M_{TX} - r_{RZ}F_{TY})/(r_{LZ} - r_{RZ}) \\ F_{LZ} &= F_{LY}tan(\theta) \textbf{ (Assumption 4)} \end{aligned} \tag{8}$$

With these four simplifying assumptions in place, it is now possible to estimate $\boldsymbol{F}_L$, $\boldsymbol{F}_R$, $\boldsymbol{r}_L$, and $\boldsymbol{r}_R$, and use those values as inputs to the multibody formulation to calculate the human system kinetics.

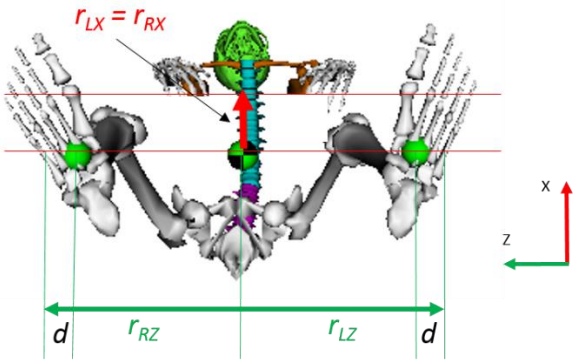

Figure 3. Assumptions 2 and 3: the Z components of r_L and r_R are a fixed distance, d, outside the centerline of the feet and the X components of r_L and r_R are equal.

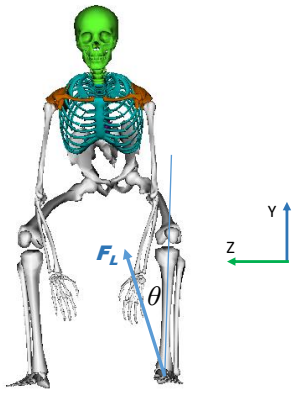

Figure 4. Assumption 4: the angle θ of F_L in the YZ plane is constant.

II. Methods

A. Participants

Four persons participated in this pilot study: two males and two females, aged 42.5±7.0 years. Inclusion criteria were ages 25-55, familiarity with resistance training, and no contraindications for resistance exercise based upon a recent physical examination. The participants' anthropometric characteristics ranged approximately from a 5th percentile female (164 cm, 51 kg) to a 95th percentile male (188 cm, 113 kg). Table 1 lists the characteristics of all four participants. After becoming familiar with the exercise device, each participant provided informed consent. The NASA Institutional Review Board approved this evaluation.

Table 1. Participant characteristics

Designator	Gender	Age (y)	Height (cm)	Body Mass (kg)
S01	Male	34	188	113
S04	Female	42	164	51
S05	Male	51	176	86
S06	Female	43	170	68

B. Experimental Setup

1. Device for Aerobic and Resistance Training (DART)

DART (TDA Research, Inc.; Wheat Ridge, CO)[15] was developed as an exercise countermeasure device to accommodate heavy resistance training (up to 180 kg) in a spaceflight environment. A computer-controlled servomotor provides the cable tension according to a user-selected loading profile. Profiles used in this work were the Free Weight (FW) loading profile, which reproduces the inertial effects of exercising with a free weight equivalent of the nominal load setting, and the Flywheel (FLY) profile, which provides the same response and feel as if the exerciser were using an inertial flywheel-based exercise device. A load cell inside the DART device measured the output cable tension force through a coupling mechanism. The DART's outer dimensions are 61 cm long x 36 cm wide x 22 cm high.

2. Exercise Protocol

Prior to data collection, an exercise physiologist evaluated each participant to determine their 3-repetition maxima (3RM). The load values used for data collection were chosen based on the participants' estimated training status[16].

For each exercise, two different DART loading profiles were used: one simulating a free weight (FW) and one simulating a flywheel device (FLY). For squats, the tether from the DART was attached to a harness (YoYo Technologies AB, Stockholm, Sweden) worn by the participant. For deadlifts, the participant grasped a knurled T-bar attachment to the tether. The knurled aluminum T-bar measured 51 cm long x 3 cm (diameter) with a mass of 3.9 kg.

All participants performed both conventional deadlifts[17] and conventional squats[18]. Participants used a dual-pronated grip for all deadlifts. Participants performed three FW sets of varying load: heavy (H, 6-8RM), medium (M, 9-11RM), and light (L, 12-15RM) based on their training status. They also performed two flywheel sets (F1, F2) where the inertia of the second trial was set to twice that of the first trial.

Each participant maintained a fixed, self-selected cadence for deadlifts (2.75±0.12 s) and squats (2.75±0.21 s) aided by a metronome. Each trial was five repetitions. An experienced athletic coach verified proper form[17,18] during data collection. Proper form promotes consistency in the effects of the assumptions across subjects.

3. Motion Capture

Data collection occurred in the Exercise Countermeasures Laboratory (ECL) at the NASA Glenn Research Center.

Motion history: A 12-camera motion analysis system (Smart-DX, BTS Bioengineering, Milan, Italy) collected the participant's motion history at 100 Hz. The system tracked the spatial position of 56 spherical reflective markers, 10 mm in diameter, placed at key anatomical sites. The system was calibrated within the participant's activity volume according to the manufacturer's procedures. Calibration error was <0.1 mm. A static pose of the participant was used to scale a biomechanical model to the participant's anthropometrics. BTS's SMARTtracker® and SMARTanalyzer® software were used to remove spurious marker trajectories, interpolate dropouts, and remove stray reflections using the manufacturer's recommended procedures.

GRF&M: Two 40- by 60-cm quartz crystal piezoelectric force plates (BTS Bioengineering P-6000) measured bilateral GRF&M at 100 Hz. The Smart-DX system synchronized the GRF&M and motion data automatically. The participant stood with the insertion point of the cable into the DART device lying between the feet and the force plates (Figure 5).

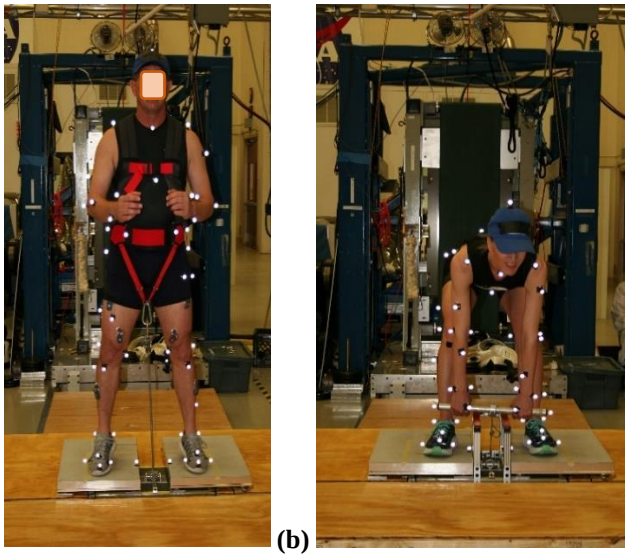

(a) (b)

Figure 5. Participant performing (a) squat and (b) deadlift resistance exercises on the DART device.

Applied external loads: A load cell (TE Connectivity, Model FC2311-0000-0250-L, Schaffhausen, Switzerland) and an integrated motor/encoder (Kollmorgen, Model AKM43L-BKCNAA-00, Radford, Virginia, USA) in line with the DART device cable recorded the time history of the applied external loads and the cable displacement, respectively, at a sampling rate of 100 Hz.

Data processing: Motion capture, GRF&M, and external loads data were filtered in MATLAB (Mathworks, Natick, Massachusetts) at 6 Hz using an 8-pole Butterworth filter.

C. Biomechanical Analysis

1. Biomechanical Modeling

An OpenSim[19] biomechanical model[20] was modified by adding two new joints to the model: a thoracic joint between vertebrae T12 and L1 and a cervical joint between C7 and T1. These new joints in the spine and neck allowed for more flexibility of the torso to properly track the kinematics of a squat or a deadlift. Torque actuators drove the new joints rather than added muscle force actuators. The modified model was scaled to each subject based on their anthropometrics and motion capture data taken during a static pose. The total squared error was <0.5 cm in the static pose during scaling and <2.5 cm for the exercises during inverse kinematics. The maximum single marker error was <5 cm.

The models contain 26 body segments for deadlift and 18 body segments (no arms) for the squat. Participants performed the squat with the arms in a fixed position. Therefore, the inertial properties of the arms in the squat models were lumped into the torso using the parallel axis theorem with the motion capture data used to locate each body segment's COM. Both the deadlift and squat models had 80 lower limb muscles.

The modeling process followed the workflow recommended in the OpenSim user documentation[19], i.e., model scaling, then inverse kinematics, and then ID. Kinetic outcomes from ID, specifically joint moments, were compared between traditional ID with measured GRF&M, and those estimated using our methodology. In both cases, a force balance methodology, as described above, was used to determine the loading vector based on the measured cable tension in the DART device and the kinematics.

2. Software Plugin

To solve for the estimated GRF&Ms, the plug-in first runs ID with zero non-gravitational external forces applied. The resulting residual force and moment, automatically calculated by OpenSim ID at the root node of the dynamics tree, must then be equal to the total non-gravitational external force and moment required to balance the system for the given trajectory and mass properties. After correcting for the offset between the root node and the system COM, these values become equal to the $(m\boldsymbol{a} - m\boldsymbol{g})$ and $d\boldsymbol{H}/d$t quantities in equation Eq. (6) above.

The second step is accomplished by an OpenSim plugin called BodyForce that is based on the Analysis Plugin Template delivered with OpenSim documentation. Analysis plugins allow OpenSim users to leverage Application

Programming Interface (API) calls to obtain body and system level kinematic states at each time step of the human trajectory. Using this information, along with $m(\boldsymbol{a}-\boldsymbol{g})$, $d\boldsymbol{H}/dt$, and the device force and POA read from a data file, BodyForce solves for the estimated GRF&Ms based on Eq. (6). The high-level flow of the plugin is as follows:

- **readDataFromFiles()**
  - Parses the residual force and moment from a file generated by ID on the subject motion with no external forces/moments applied
  - Parses the device force ($\boldsymbol{F}_{\mathrm{d}}$)and POA ($\boldsymbol{r}_d$) from a file containing processed exercise device and motion capture data from the trial
- **getBodyKinematics()**
  - OpenSim API calls obtain pertinent body level kinematics (i.e., bar and foot positions)
- **getSystemKinematics()**
  - OpenSim API calls obtain the system kinematics (i.e., system COM position)
  - Calculates $m(\boldsymbol{a}-\boldsymbol{g})$ and $d\boldsymbol{H}/dt$ from the raw no-force ID residual force and moment
- **estimateGRF&Ms()**
  - Using the previous data, and the simplifying assumptions, solves for the $\boldsymbol{F}_L$, $\boldsymbol{F}_R$, $\boldsymbol{r}_L$, and $\boldsymbol{r}_R$ that balance Eq. (6)
- **writeExternalForcesToFile()**
  - Output the "balanced" device and GRF&Ms to a file for use with ID

D. Analytical Methods

Joint moments were plotted as ensemble averages, time-normalized to 101 samples from 0 (repetition start) to 1.0 (repetition completion) in increments of 0.01 with the area between ±1 standard deviation (SD) shaded. Peak moments were defined as the values of the greatest magnitude (positive or negative) on the joint moment trajectories. Joint moment impulses were defined as the time integrals under the joint moment trajectory curves. RMSEs were computed as in Ren, et al.[11], whereby the estimated joint moments were compared with an ID solution based on the measured force plate data.

The Pearson correlation coefficient (r) was calculated and was categorized (in absolute value) as $r \leq 0{:}35$, $0{:}35 < r \leq 0.67$, $0.67 < r \leq 0.9$, $0.9 < r$ to be weak, moderate, strong, or excellent correlation, respectively (following Taylor[21]). Further differences were quantified using the Sprague and Geers curve phase (P) and magnitude (M) difference[22,23]. The metrics P and M, expressed as percentages, are designed to produce a zero value when the curves are identical; therefore, a lower value indicates better agreement between trajectories. Computing RMSE, r, P, and M allowed for direct comparison with results of similar studies.

III. Results

A. Quantifying the Assumption Effects for Squat and Deadlift Exercises

1. Zero Ground Reaction Moments

Peak measured ground reaction moments on both feet for all participants for all trials are shown in Figure 6. In all cases, the highest measured ground reaction moment is the so-called "free moment", M_{Y}, which never exceeded 0.02 N-m/(BWF*BH) for any participant. Errors resulting from the negligible moments assumption would therefore be expected to produce a small effect on both sagittal plane kinetics as well as non-sagittal plane kinetics.

2. Equal Fore-Aft Positions for the X Location of the POAs

The RMSE between the X (fore-aft) components of the measured GRFs of both feet vs. the estimated values are shown for all trials in Figure 7. For all participants, the RMSE in the fore-aft force component was <0.04 N/BWF. The assumption of equal values of POA_{X} for both feet affects the sagittal plane kinetics almost exclusively, and the resulting errors were an order of magnitude or more less that the kinetic outcomes of interest.

3. Fixed Position of the Z Location of the POAs and Fixed Y-Z Plane Angle for the F_z Vector

The measured Z location of the POAs ranged from 0.7 to 3.6 cm (squat) or from 1.4 to 3.1 cm (deadlift) outside the midline of the foot across all four subjects. The measured values for the angle θ ranged from 6.0º to 10.8º (squat) or 4.0º to 10.9º (deadlift). The RMSE between the Z (lateral) components of the measured GRFs of both feet vs. the estimated values are shown for all trials in Figure 8. For all participants, the worst case in the lateral force component ranged from 0.05-0.07 N/BWF. These values were comparable in magnitude to the non-sagittal plane kinetics of interest, such that the assumptions of fixed location for $\mathrm{POA_Z}$ and fixed angle for F_Z in the Y-Z plane would be expected to create significant errors in non-sagittal plane kinetics.

B. Effect on Squat Exercise Kinetics

Typical normalized joint moment trajectories in the sagittal plane for the squat exercise are shown in Figure 9. The plots compare the trajectories with and without measured GRF&M using the free weight (FW) profile and the medium (M) load. The trajectories compared favorably; both trajectories had the same qualitative shape and small differences across the entire movement.

Typical normalized joint moment trajectories outside the sagittal plane for the squat exercise are shown in Figure 10. The plots compare the trajectories with and without measured GRF&M using the FW profile and the M load. The trajectories compared less favorably than the sagittal plane joints; the trajectories no longer had the same qualitative shape and larger differences were seen across the entire movement.

Figure 11 compares the percent change in joint moment impulse when kinetics are computed with and without measured GRF&M data for both the sagittal plane joints and the non-sagittal plane joints. Much higher differences were observed in the non-sagittal joints compared with the sagittal joints.

C. Effect on Deadlift Exercise Kinetics

Typical normalized joint moment trajectories in the sagittal plane for the deadlift exercise are shown in Figure 12. The plots compare the trajectories with and without measured GRF&M using the FW profile and the M load. The trajectories compared favorably; both trajectories had the same qualitative shape and small differences across the entire movement, although the trajectories did appear to have larger differences than the squat exercise.

Typical normalized joint moment trajectories outside the sagittal plane for the squat exercise are shown in Figure 13. The plots compare the trajectories with and without measured GRF&M using the FW profile and the M load. The trajectories compared less favorably than the sagittal plane joints; the trajectories did not have the same qualitative shape and larger differences were seen across the entire movement. These differences appeared to be much larger than those seen for the squat exercise.

Figure 14 compares the percent change in joint moment impulse (i.e., the area under the moment vs. time curve) when kinetics are computed with and without measured GRF&M data for both the sagittal plane joints and the non-sagittal plane joints. Much higher differences were observed in the non-sagittal joints compared with the sagittal joints.

Table 2 also indicates that a better estimation of kinetics occurs in the sagittal plane joints (*P* ranging from 0.0% to 1.7%, *M* ranging from -8.5% to 19.8% and *r* ranging from 0.583 to 1.000) vs. the non-sagittal joints (*P* ranging from 2.9% to 68.6%, *M* ranging from -64.1% to 301.7% and *r* ranging from 0.273 to 0.967). In general, the squat exercise kinetic estimates were more robust than those of the deadlift, based on notably lower values for *P* and *M*, and notably higher values of *r* for most joints.

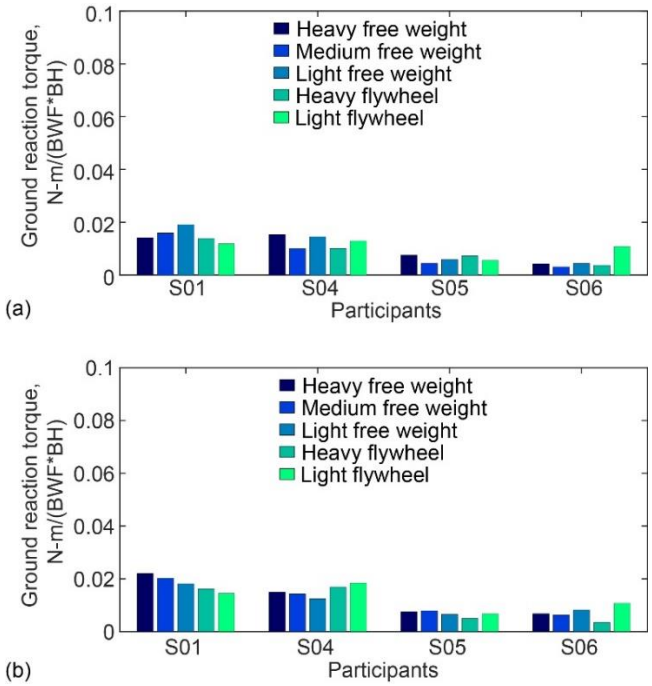

Figure 6. Peak values of measured ground reaction torque during the deadlift exercise for the left (a) and right (b) feet.

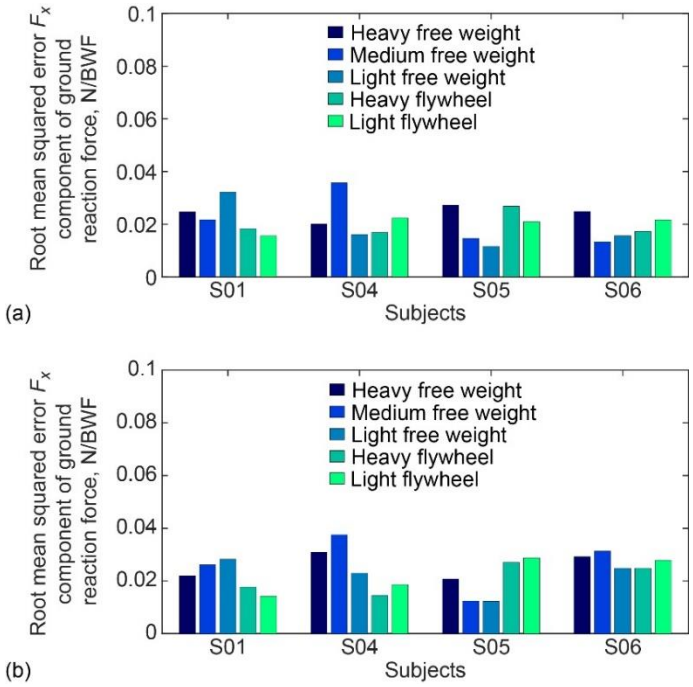

Figure 7. RMSE values between measured F_x components of the GRF during the deadlift exercise for the left (a) and right (b) feet.

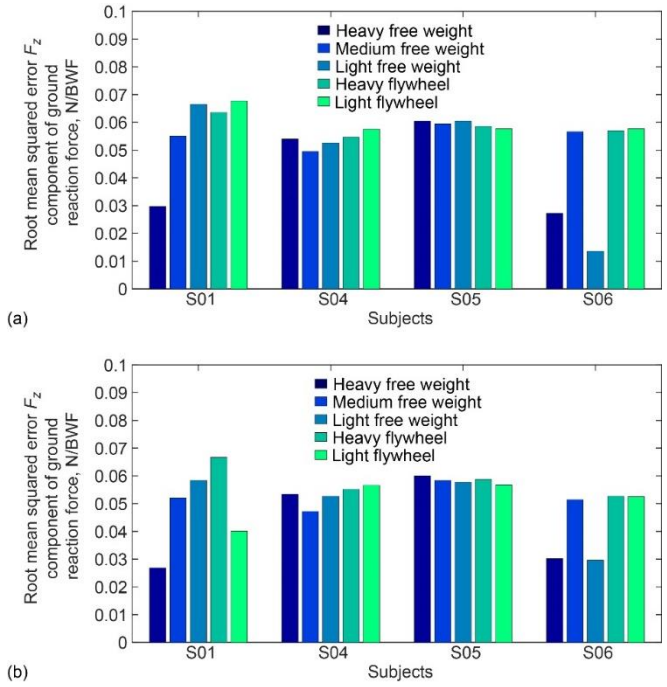

Figure 8. RMSE values between measured F_z components of the GRF during the deadlift exercise for the left (a) and right (b) feet.

Table 2. Comparison of joint moment trajectories computed with vs. without measured GRF&M using curve phase (P) and magnitude (M) difference (mean(SD)) and Pearson correlation coefficient *r* averaged over all participants.

	Joint	Squat					Deadlift				
		P (%)		M (%)		*r*	P (%)		M (%)		*r*
Sagittal Joints	Hip Flexion L	0.7	(0.20)	-7.1	(1.20)	0.999	1.1	(0.30)	-0.6	(2.00)	0.997
	Knee Flexion L	1.5	(0.70)	9.8	(2.30)	1.000	5.0	(1.40)	19.8	(2.60)	0.991
	Ankle Dorsiflexion L	0.4	(0.10)	-5.7	(1.20)	0.998	2.5	(0.90)	-8.5	(2.90)	0.801
	Hip Flexion R	0.7	(0.20)	8.4	(1.80)	0.999	1.5	(0.80)	6.6	(3.10)	0.995
	Knee Flexion R	1.7	(0.50)	-2.3	(1.30)	0.999	4.6	(2.00)	6.3	(4.20)	0.988
	Ankle Dorsiflexion R	0.6	(0.10)	3.8	(2.10)	0.998	3.5	(0.60)	11.6	(3.60)	0.583
	Lumbar Extension	0.0	0.00	0.0	0.00	1.000	1.0	(0.30)	3.4	(2.00)	0.993
Non-sagittal Joints	Hip Adduction L	24.7	(17.00)	-4.4	(45.30)	0.767	47	(16.00)	-68	(11.30)	0.303
	Hip Internal Rotation L	11	(2.90)	-55.5	(8.50)	0.929	52.5	(18.40)	176.5	(36.00)	0.273
	Subtalar Inversion L	2.9	(0.80)	-9.9	(9.20)	0.956	5.1	(2.10)	-7.8	(10.90)	0.761
	Hip Adduction R	8.5	(3.50)	15.9	(32.50)	0.807	68.6	(6.90)	25.1	(39.20)	0.412
	Hip Internal Rotation R	19.8	(4.10)	-64.1	(7.50)	0.851	39.7	(15.80)	301.7	(53.00)	0.648
	Subtalar Inversion R	3.0	(0.80)	7.8	(9.10)	0.967	6.0	(3.50)	-4.0	(14.50)	0.621

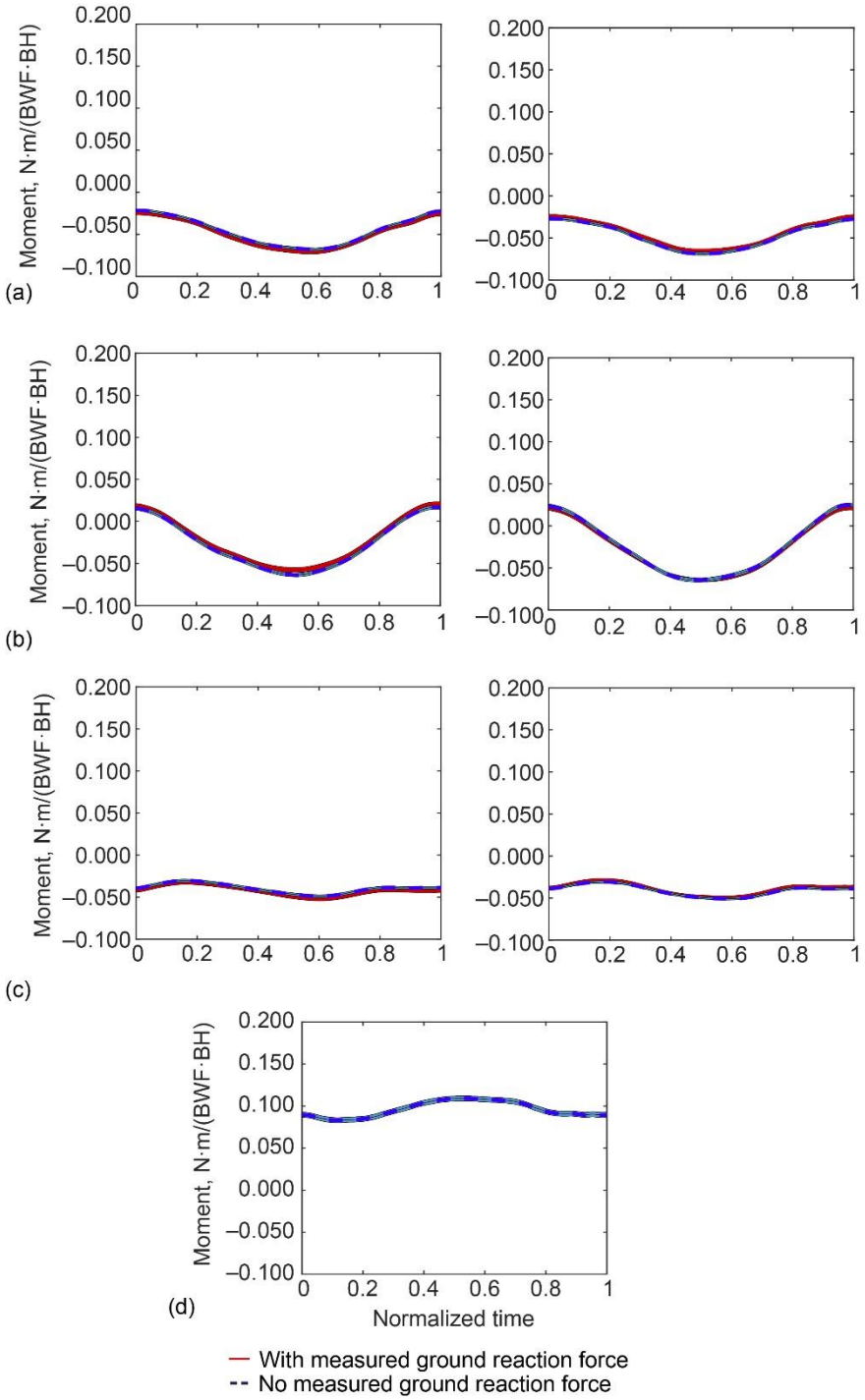

Figure 9. Normalized joint moment trajectories, with (red, solid) and without (blue, dashed) measured GRF&M, compared in the sagittal plane for the squat exercise, for the medium FW loading profile, averaged for all reps and all participants for (a) left and right hip flexion moment, (b) left and right knee flexion moment, (c) left and right ankle dorsiflexion moment, and (d) lumbar extension moment. Flexion moments in the limbs that are negative indicate net joint extension.

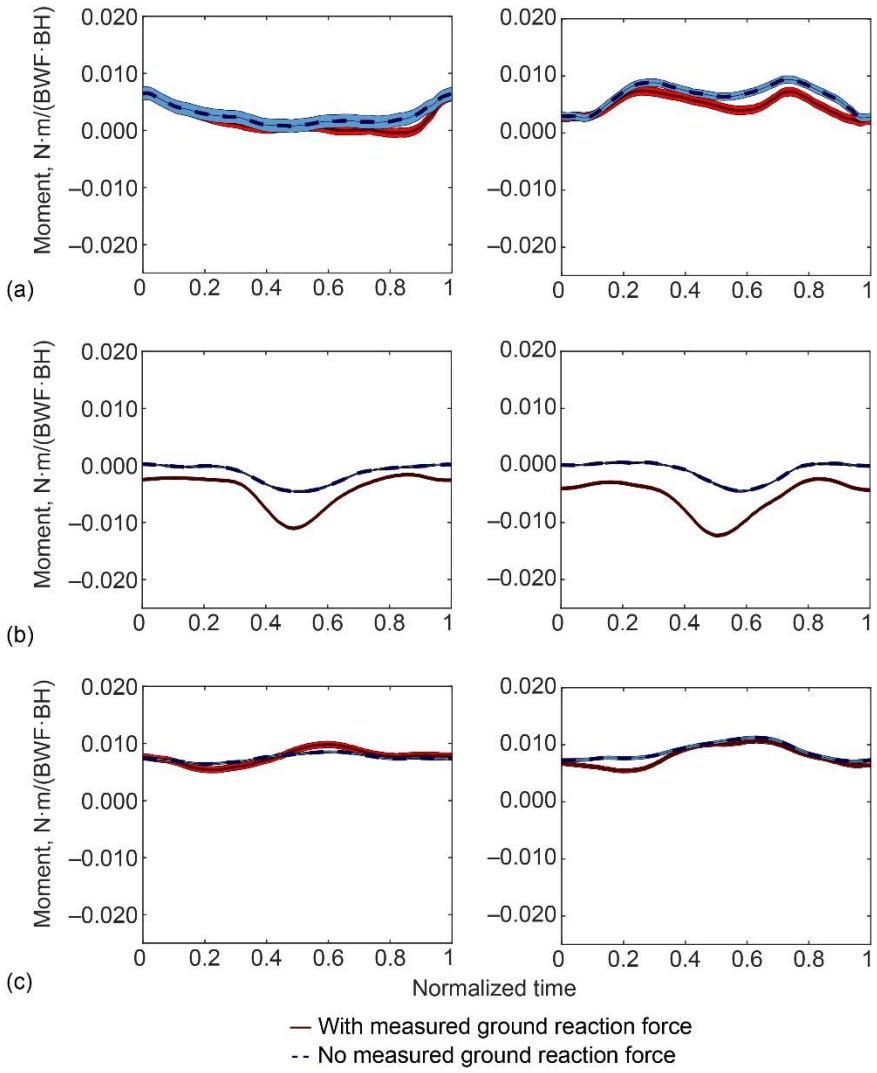

Figure 10. Normalized joint moment trajectories, with (red, solid) and without (blue, dashed) measured GRF&M, compared outside the sagittal plane for the squat exercise, for the medium FW loading profile, averaged for all reps and all participants for (a) left and right hip adduction moment, (b) left and right hip internal rotation moment, and (c) left and right ankle subtalar inversion moment.

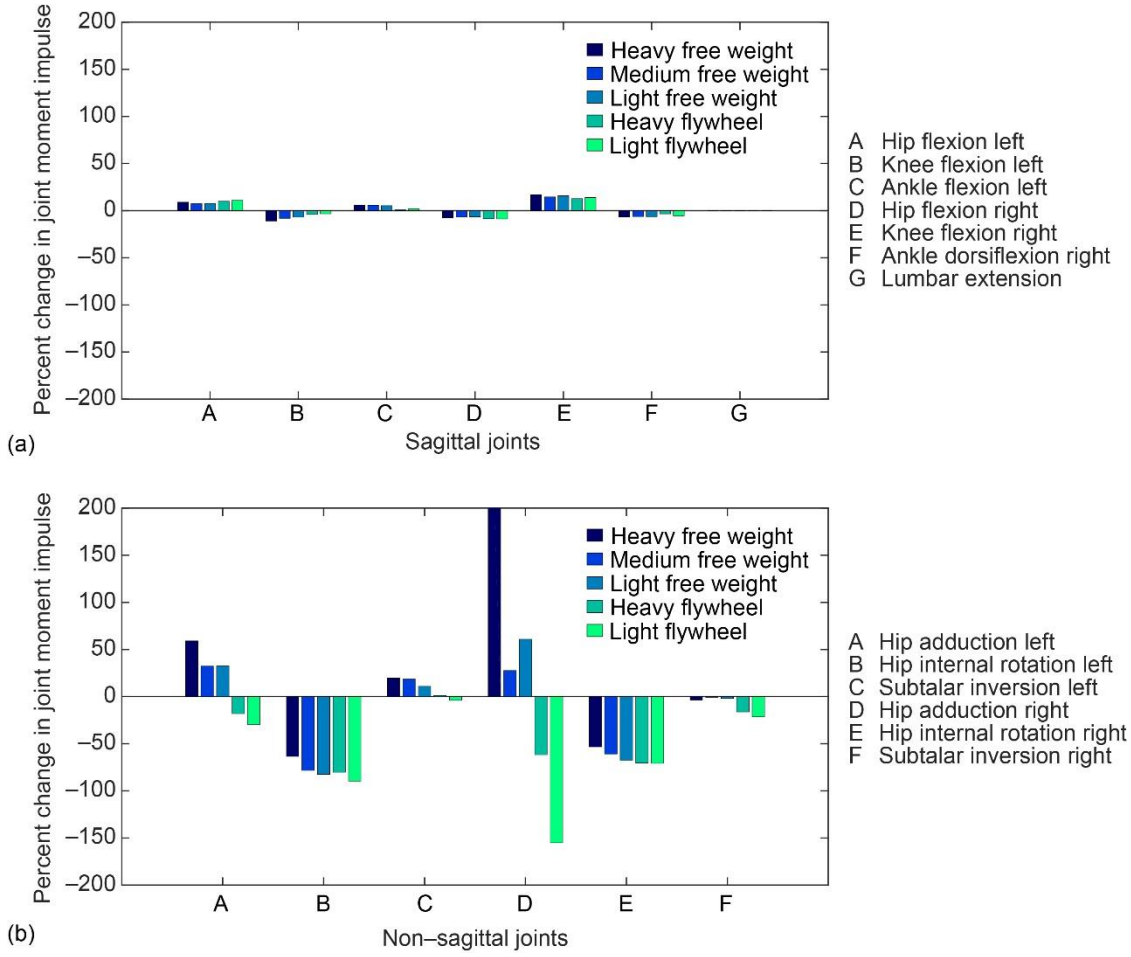

Figure 11. Percent change in joint moment impulse for the squat exercise, with and without measured GRF&M for (a) sagittal plane and (b) non-sagittal plane joints, for all trials averaged over all participants.

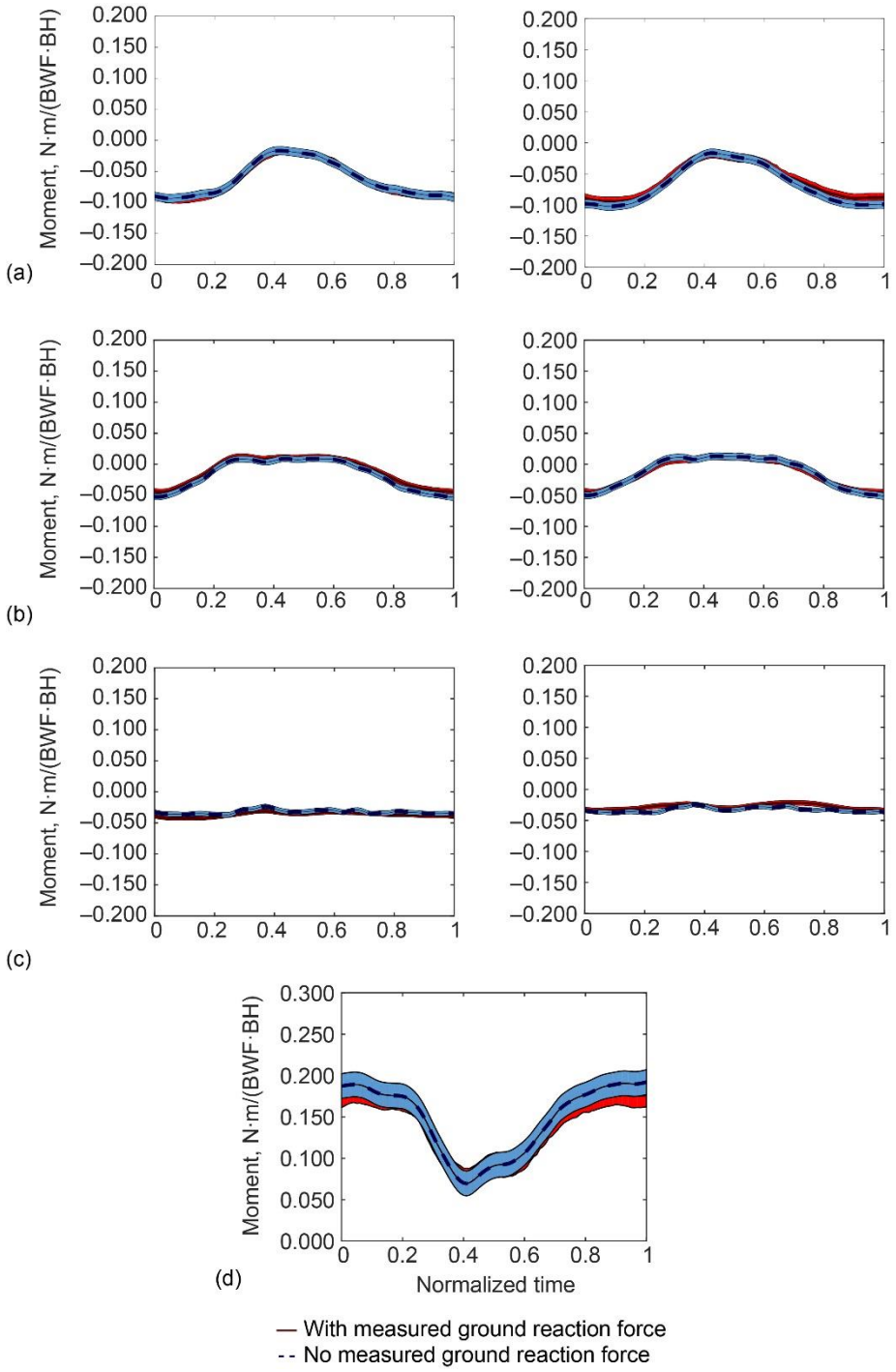

Figure 12. Normalized joint moment trajectories, with (red, solid) and without (blue, dashed) measured GRF&M, compared in the sagittal plane for the deadlift exercise, for the medium FW loading profile, averaged for all reps and all participants for (a) left and right hip flexion moment, (b) left and right knee flexion moment, (c) left and right ankle dorsiflexion moment, and (d) lumbar extension moment. Flexion moments in the limbs that are negative indicate net joint extension.

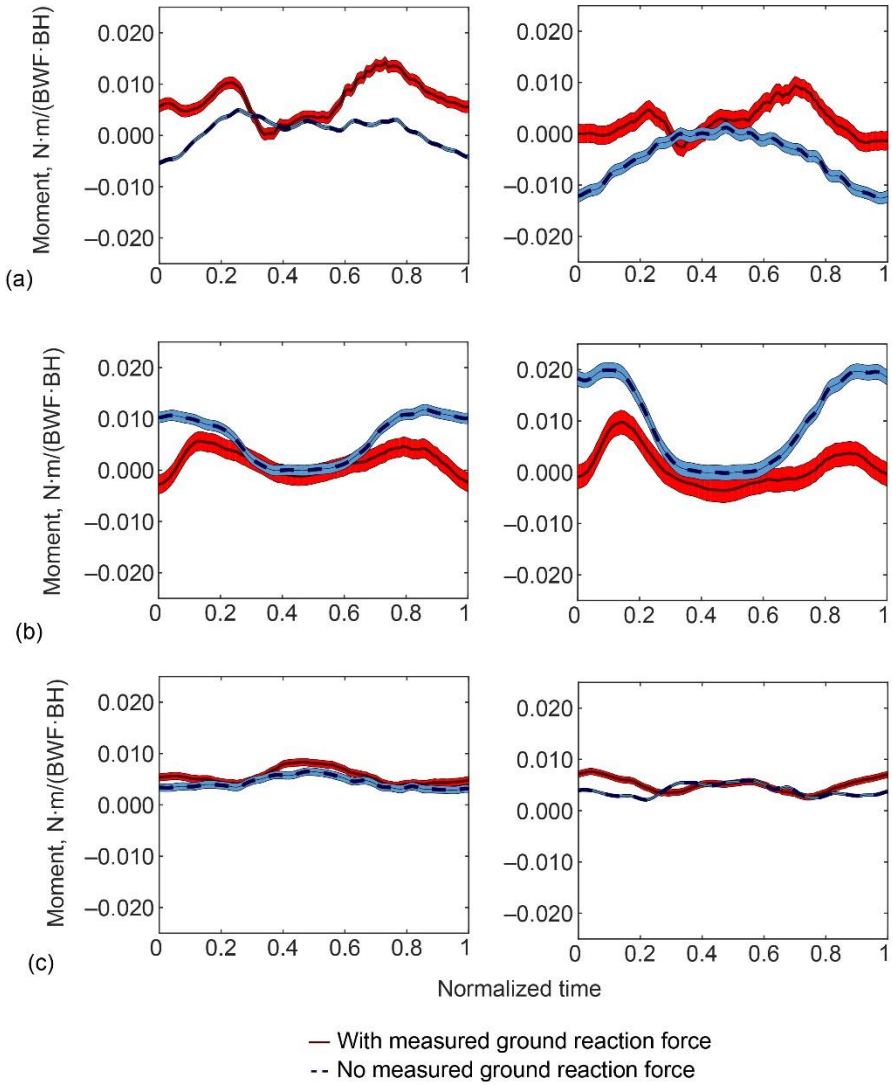

Figure 13. Normalized joint moment trajectories, with (red, solid) and without (blue, dashed) measured GRF&M, compared outside the sagittal plane for the deadlift exercise, for the medium FW loading profile, averaged for all reps and all participants for (a) left and right hip adduction moment, (b) left and right hip internal rotation moment, and (c) left and right ankle subtalar inversion moment.

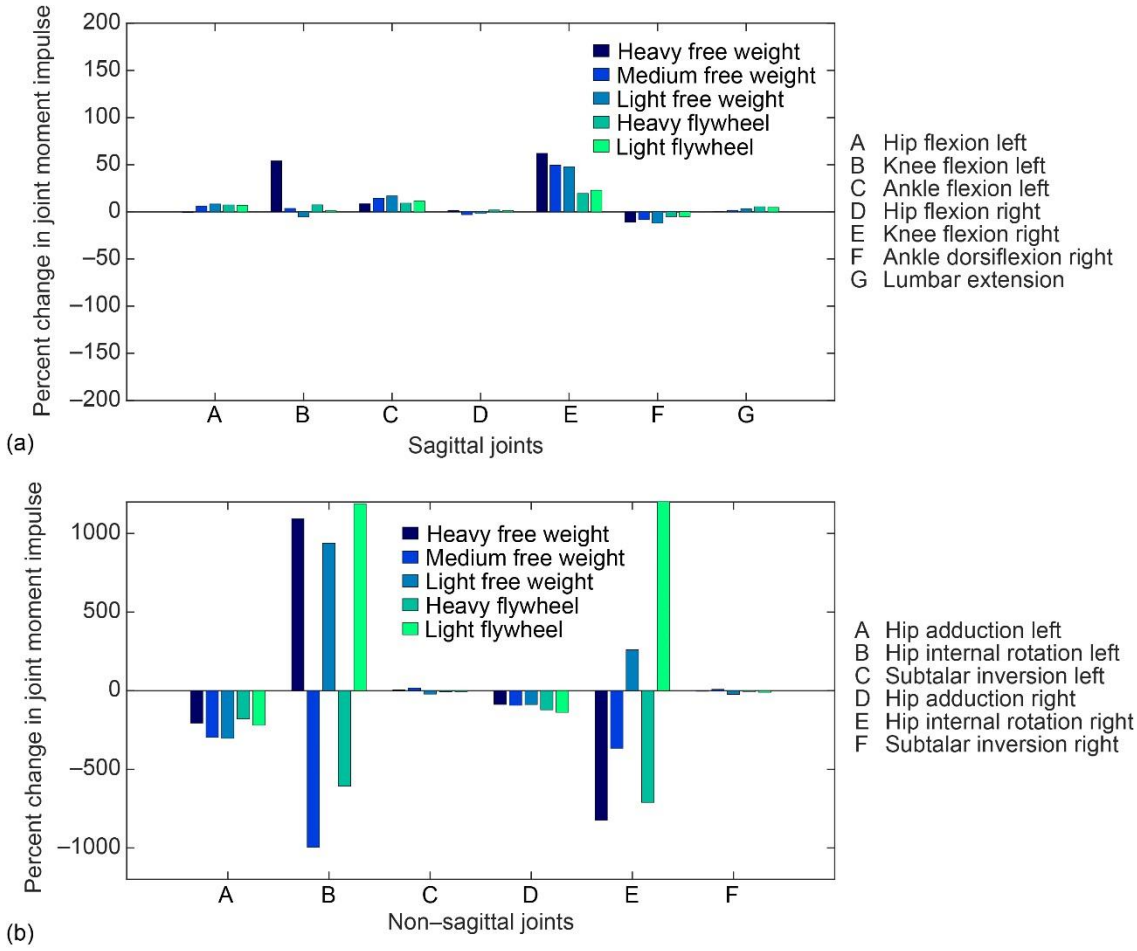

Figure 14. Percent change in joint moment impulse for the deadlift exercise, with and without measured GRF&M for (a) sagittal plane and (b) non-sagittal plane joints, for all trials averaged over all participants.

IV. Discussion

It is apparent that the simplifying assumptions made to reduce the number of unknowns (when GRF&M are not measured) have a much larger impact on the kinetics outside the sagittal plane than kinetics within the sagittal plane. Fixing both the Z component of the POA and the angle θ that the GRF vector makes with the vertical axis induces greater error than forcing the X component of the POA to be the same on both feet. The effect of zeroing the ground reaction moments appears to be quite small in both planes. The smaller magnitude of the non-sagittal plane moments relative to the sagittal plane moments (i.e., up to one order of magnitude lower) is also a contributing factor to these findings.

The main advantage of this methodology is its simplicity. There are no required changes to the model, such as additional contact surfaces; no additional instrumentation required, such as pressure insoles or IMS sensors; and no need to code additional optimization routines. The straightforward OpenSim plugin simply computes a new external forces file with the assumptions in place. Then, traditional ID analysis proceeds from there.

The main disadvantages are 1) that this methodology is very motion-specific to lower body resistance training, because the assumptions arise from empirical knowledge of these movements, 2) that it is mostly unable to provide meaningful estimates of joint moments outside the sagittal plane, and 3) that kinematic data of reasonable quality are required as inputs to the model. However, for any further study of sagittal plane-based resistance training where GRF&M are not measured, and where kinematic data exist, this methodology has potential applications and may provide useful estimates of the sagittal plane kinetics.

It would be most informative to compare our findings directly with other reported methods for calculating the kinetics of the squat and deadlift movements without measured GRF&M. Unfortunately, there is not a large established base of literature in this area from which to draw comparisons; however, the following provides some insight.

Fluit et al.[9] employed a contact model with optimization and studied several movements including a body weight deep squat. The sagittal plane results for estimated vs. computed moments (Table 2) compare more favorably than their results (hip flexion moment: M = 5.5%, P = 4.6%, and r = 0.967; knee flexion moment: M = 5.4%, P = 12.3%, and r = 0.733; and ankle dorsiflexion moment: M = 28.7%, P = 11.7%, and r = 0.603), although their non-sagittal plane results are much more favorable than these results. Whereas the qualitative comparisons of the joint moment trajectories in this work show excellent agreement in the sagittal plane and generally unsatisfactory agreement outside of it, their similar qualitative comparisons are in fairly good agreement throughout. Robert et al.[8] use the same contact model methods for sit-to-stand maneuvers, and they report RMSE values generally <10% in the sagittal plane, as does this work.

Bonnet et al.[24] also studied a body weight squatting movement with a constrained external Kalman filter to estimate GRF&M. They report normalized RMSE values and r values in the sagittal plane (ankle: RMSE = 33.9±17.2%, r = 0.74±0.13; knee: RMSE = 39±19.7%, r = 0.94±0.07; hip: RMSE = 59.6±28.5%, r = 0.77±0.24; lumbar: RMSE = 56.3±37.6%, r = 0.78±0.23) that our methodology surpasses (see Figure 9, Table 2).

We believe that this is the first study that estimates kinetic outcomes for the deadlift movement without measuring GRF&M. There are numerous studies of human gait and gait-based movements that estimate kinetics without measuring GRF&M (cf.[1,2,10,14,25,26]) with RMSE and r values generally in agreement with this work for resistance training.

This method demonstrates that with simplifying assumptions based on empirical knowledge of the motion under study, and an interest in only those outcomes that lie in the primary plane of motion, useful kinetic estimates may be obtained without modifications to the human model, without additional instrumentation and without computationally intensive optimization code. As the squat and deadlift provide most of their training benefit to muscles that articulate in the sagittal plane, we believe that the models still produce operationally relevant and useful information.

Further improvements to this methodology could be gained by optimizing the selection of the Z component of the foot COP and the angle θ based on the anthropometrics of the human exerciser. This would require collecting a larger data set from a wide sampling of persons of various sizes and performing ID followed by a regression analysis on those data. Additionally, it is possible that adding some limited amount of measured data could eliminate the need for some of the assumptions. For instance, force shoes, while not typically giving reliable force vector measurement, might provide reasonably accurate POA data that would eliminate the need for assumptions 2 and 3. Future work focused on performing sensitivity analyses to determine how the individual assumptions propagate through the model and on reintroducing measurements selectively to omit the most sensitive assumption would produce an even more refined methodology.

V. Conclusion

This work describes a method for computing lower body kinetics during the deadlift and squat exercises in the absence of measured ground reaction forces and moments (GRF&M) using kinematic information from motion capture and load profile history data from the exercise device. The method relies on empirically-based assumptions about these movements that reduce the number of unknowns in the multibody inverse dynamics (ID) equations of motion. This method estimates kinetics in the sagittal plane with relatively low error compared with traditional ID analysis using force plate data, but not nearly as well in the non-sagittal planes. We concluded that this is because 1) the assumptions themselves are made primarily about the values of force components outside the sagittal plane, and 2) the non-sagittal plane kinetics are about a full order of magnitude in value below the sagittal plane kinetics and are, therefore, more prone to error.

This work is important because it allows the use of freely available biomechanical models without modification, optimization, or the addition of complex contact surfaces, and without any additional instrumentation, to analyze sagittal plane kinetics of resistance training movements. The OpenSim plugin produces a modified external force file, from which ID analysis may proceed in the traditional fashion.

Acknowledgments

This work is performed by the Cross-cutting Computational Modeling Project (CCMP) managed out of the NASA Glenn Research Center by Kelly M. Gilkey. The project is funded by the NASA Human Research Program (HRP) managed out of the NASA Johnson Space Center. The CCMP project directly supports the Program Science Management Office of HRP.

References

[1]Chumanov, E. S., Remy, C. D., and Thelen, D. G., "HHS Public Access," 2015, pp. 1–21.

[2]Jacobs, D. A., and Ferris, D. P., "Estimation of Ground Reaction Forces and Ankle Moment with Multiple Low-Cost Sensors," *J. Neuroeng. Rehabil.,* 2015, pp. 1–12.

[3]Jung, Y., Jung, M., Lee, K., and Koo, S., "Ground Reaction Force Estimation Using an Insole-Type Pressure Mat and Joint Kinematics During Walking Vertical Reaction," *J. Biomech.,* Vol. 47, No. 11, 2014, pp. 2693–2699.

[4]Faber, G. S., Chang, C. C., Kingma, I., Dennerlein, J. T., and van Dieën, J. H., "Estimating 3D L5/S1 Moments and Ground Reaction Forces During Trunk Bending Using a Full-Body Ambulatory Inertial Motion Capture System," *J. Biomech.,* Vol. 49, No. 6, 2016, pp. 904–912.

[5]Karatsidis, A., et al.: "Estimation of Ground Reaction Forces and Moments During Gait Using Only Inertial Motion Capture," *Sensors,* Vol. 17, No. 1, 2017, pp. 1–22.

[6]Logar, G., and Munih, M., "Estimation of Joint Forces and Moments for the In-Run and Take-Off in Ski Jumping Based on Measurements with Wearable Inertial Sensors," *Sensors,* Vol. 15, No. 5, 2015, pp. 11258–11276.

[7]Audu, M. L., Kirsch, R. F., and Triolo, R. J., "Experimental Verification of a Computational Technique for Determining Ground Reactions in Human Bipedal Stance," *J. Biomech.,* Vol. 40, No. 5, 2007, pp. 1115–1124.

[8]Robert, T., Causse, J., and Monnier, G., "Estimation of External Contact Loads Using an Inverse Dynamics and Optimization Approach: General Method and Application to Sit-to-Stand Maneuvers," *J. Biomech.,* Vol. 46, No. 13, 2013, pp. 2220–2227.

[9]Fluit, R., Andersen, M. S., Kolk, S., Verdonschot, N., and Koopman, H. F., "Prediction of Ground Reaction Forces and Moments During Various Activities of Daily Living," *J. Biomech.,* Vol. 47, No. 10, 2014, pp. 2321–2329.

[10]Skals, S., Jung, M. K., Damsgaard, M., and Andersen, M. S., "Prediction of Ground Reaction Forces and Moments During Sports-Related Movements," *Multibody Syst. Dyn.,* Vol. 39, No. 3, 2017, pp. 175–195.

[11]Ren, L., Jones, R. K., and Howard, D., "Whole Body Inverse Dynamics Over a Complete Gait Cycle Based Only on Measured Kinematics," *J. Biomech.,* Vol. 41, No. 12, 2008, pp. 2750–2759.

[12]Hackney, K. J., et al., "The Astronaut-Athlete: Optimizing Human Performance in Space," *J. Strength Cond. Res.,* Vol. 29, No. 12, 2015, pp. 3531–3545.

[13]Schneider, S. M., et al., "Training with the International Space Station Interim Resistive Exercise Device," *Med. Sci. Sports Exerc.*, vol. 35, no. 11, 2003, pp. 1935–1945.

[14]Dijkstra, E. J., and Gutierrez-Farewik, E. M., "Computation of Ground Reaction Force Using Zero Moment Point," *J. Biomech.,* Vol. 48, No. 14, 2015, pp. 3776–3781.

[15]Bruinsma, D., "Device for Aerobic and Resistive Training—Final Report," NASA SBIR Contract NNX14CC97P, TDA Res. Inc., Wheat Ridge, CO, December 2014.

[16]Brzycki, M., "Strength Testing—Predicting a One-Rep Max from Reps-to-Fatigue," *J. Phys. Educ. Recreat. Dance,* Vol. 64, No. 1, 1993, pp. 88–90.

[17]Escamilla, R. F., et al., "A Three-Dimensional Biomechanical Analysis of Sumo and Conventional Style Deadlifts," *Med. Sci. Sport. Exer.*, Vol. 32, No. 7, 2000, pp. 1265–1275.

[18]Escamilla, R. F., "Knee Biomechanics of the Dynamic Squat Exercise," *Med. Sci. Sports Exerc.,* Vol. 33, No. 1, 2001, pp. 127–141.

[19]Seth, A., Sherman, M., Reinbolt, J. A., and Delp, S. L., "OpenSim: A Musculoskeletal Modeling and Simulation Framework for In Silico Investigations and Exchange," *Procedia IUTAM,* Vol. 2, 2011, pp. 212–232.

[20]Rajagopal, A., et al., "Full Body Musculoskeletal Model for Muscle-Driven Simulation of Human Gait," *IEEE Trans. Biomed. Eng.*, Vol. 63, No. 10, 2016, pp. 2068–2079.

[21]Taylor, R., "Interpretation of the Correlation Coefficient: A Basic Review," *J. Diagnostic Med. Sonogr.,* Vol. 6, No. 1, 1990, pp. 35–39.

[22]Schwer, L. E., "Validation Metrics for Response Histories: Perspectives and Case Studies," *Eng. Comput.,* Vol. 23, No. 4, 2007, pp. 295–309.

[23]Sprague, M. A., and Geers, T. L., "Spectral Elements and Field Separation for an Acoustic Fluid Subject to Cavitation," *J. Comput. Phys.*, Vol. 184, No. 1, 2003, pp. 149–162.

[24]Bonnet V, Mazza C, Fraisse P, Cappozzo A. Real-time estimate of body kinematics during a planar squat task using a single inertial measurement unit. *IEEE Trans Biomed Eng*. 2013;60(7):1920-1926.

[25]Bonnet, V., et al., "A Constrained Extended Kalman Filter for the Optimal Estimate of Kinematics and Kinetics of a Sagittal Symmetric Exercise" *J. Biomech.,* Vol. 62, 2017, pp. 140–147.

[26]Eltoukhy, M., Kuenze, C., Andersen, M. S., Oh, J., and Signorile, J., "Prediction of Ground Reaction Forces for Parkinson's Disease Patients Using a Kinect-Driven Musculoskeletal Gait Analysis Model," *Med. Eng. Phys.,* vol. 50, 2017, pp. 75–82.

[27]Jung, Y., Ryu, J., Yoon, S., Park, S-K, and Koo, S., "Estimating Knee Adduction Moment From Joint Kinematics and Foot Pressure: Validation Using Force Plate Embedded Treadmill," *ORS (Orthopaedic Research Society) 2014 Annual Meeting,* New Orleans, LA, Table, 2014.